



ARTICLE

Development and Characterization of Eco-Friendly Non-Isocyanate Urethane Monomer from *Jatropha curcas* Oil for Wood Composite Applications

Samsul Bhakri¹, Muhammad Ghozali^{2,*}, Edy Cahyono¹, Evi Triwulandari², Witta Kartika Restu², Nissa Nurfajrin Solihat³, Apri Heri Iswanto^{4,5}, Petar Antov⁶, Viktor Savov⁶, Lee Seng Hua⁷, Erika Ayu Agustiany⁸, Lubos Kristak⁹ and Widya Fatriasari^{3,*}

¹Department of Chemistry, Universitas Negeri Semarang, Semarang, 50229, Indonesia

²Research Center for Chemistry, National Research and Innovation Agency (BRIN), Serpong, 15314, Indonesia

³Research Center for Biomass and Bioproducts, National Research and Innovation Agency (BRIN), Cibinong, 16911, Indonesia

⁴Department of Forest Product, Faculty of Forestry, Universitas Sumatera Utara, Medan, 20155, Indonesia

⁵JATI-Sumatran Forestry Analysis Study Center, Medan, 20155, Indonesia

⁶Faculty of Forest Industry, University of Forestry, Sofia, 1797, Bulgaria

⁷Laboratory of Biopolymer and Derivatives, Institute of Tropical Forestry and Forest Product, Universiti Putra Malaysia, Selangor, 43400, Malaysia

⁸Department of Forest Products, Faculty of Forestry and Environment, IPB University, Bogor, 16680, Indonesia

⁹Faculty of Wood Sciences and Technology, Technical University in Zvolen, Zvolen, 96001, Slovakia

*Corresponding Authors: Muhammad Ghozali. Email: muhammad.ghozali@brin.go.id; Widya Fatriasari. Email: widya.fatriasari@biomaterial.lipi.go.id; widy003@brin.go.id

Received: 12 April 2022 Accepted: 01 May 2022

ABSTRACT

The aim of this research work was to evaluate the potential of using renewable natural feedstock, i.e., *Jatropha curcas* oil (JCO) for the synthesis of non-isocyanate polyurethane (NIPU) resin for wood composite applications. Commercial polyurethane (PU) is synthesized through a polycondensation reaction between isocyanate and polyol. However, utilizing toxic and unsustainable isocyanates for obtaining PU could contribute to negative impacts on the environment and human health. Therefore, the development of PU from eco-friendly and sustainable resources without the isocyanate route is required. In this work, tetra-n-butyl ammonium bromide was used as the activator to open the epoxy ring with 3-Aminopropyltriethoxysilane as a catalyst to yield urethane of JCO (UJCO). The UJCO were characterized by Fourier Transform Infra-Red spectroscopy (FTIR) and their oxirane, and hydroxyl values were measured. The result showed that a decrease in oxirane value was found while the hydroxyl value was increased during the time, confirming that the urethane group was formed. The presence of functional groups in FTIR spectra at wave numbers 1732.08, 1562.34, and 3348.42 cm^{-1} indicates the functional groups of C = O (urethane carbonyl), -NH, and -OH, respectively confirmed this finding. The potential applications of NIPU in the wood composite were also outlined.

KEYWORDS

Jatropha curcas oil; urethane groups; non-isocyanate polyurethane; epoxidized JCO; cyclic carbonate; oxirane value; wood composites



1 Introduction

Polyurethanes (PU) are one of the most versatile polymer groups because they can be converted to various polymeric-based products for a wide range of industrial applications, i.e., packaging, elastomer materials, automotive parts, thermal insulation, sealant, coatings, lighting industry, biomedical applications, footwear, construction, bedding, metallurgy, furniture, adhesives, foams, and paints [1–3]. The multiple commercial applications of PU are due to their great hardness, biocompatibility, mechanical strength, and elongation properties [4,5]. In coating applications such as food, metal, and high-gloss aircraft finishes, PU is utilized because of its excellent resistance to chemicals [1]. Even though the use of PU for the development of wood adhesives is still rather limited, PU-based adhesives exhibit strong bonding characteristics such as flexibility, good adhesion, and fast curing [6–8]. PU is typically formed by the polycondensation reaction of di/poly-isocyanates and hydroxyl groups in di/polyol; as a result, the urethane functional group is identified in the main chain [9,10]. However, using isocyanate monomers is a non-environmentally friendly and toxic issue, causing serious environmental and human health-related problems, such as irritation of the eyes, respiratory and gastrointestinal tract, and asthma in the long term [11,12]. Therefore, the industrial interest has been shifted to the use of new biodegradable and renewable green resources as PU materials. Vegetable oils, including *Jatropha curcas* oils (JCO), are viable biological bioresources for the coating industry due to their low toxicity, relatively low cost, abundance, renewability, and other social and economic advantages [10,13,14]. As a result, it represents a feasible option as an epoxide starter oil [14]. Oils are fatty acid triglycerides with long aliphatic chains that give the coatings their extreme flexibility [15].

Some investigations are still exploiting JCO as a material for the synthesis of biodiesel components and lubricants that are contributed by the favorable low-temperature viscosity (below 25°C) and acidic properties, which are lower than other vegetable oils, such as linseed, castor, and soybean oil [16–18]. Compared with other vegetable oils, JCO has greater potential as industrial raw material because it is a highly-available and non-edible feedstock that could even cause poisoning when consumed [19,20]. Furthermore, it can grow well on poor soil and has good resistance to drought with a long period of seed production (up to 50 years). It is less expensive than other vegetable oils such as rapeseed oil and soybean oil [19,21]. Due to its relatively high unsaturated fatty acid content and excellent oxidation stability, JCO is a suitable material for the development of non-isocyanate PU (NIPU), including adhesive, alkyd epoxy resin, surface coating, food packaging, and nanocomposites [22]. In addition, it has a high iodine value (105 gI₂/100 g) as a representation of unsaturation or double bonds content [20,23] with an unsaturated fatty acid fraction of 0.78–0.79.

Concerning environmental protection and human health and safety, sustainable and efficient alternative methods for the synthesis of NIPU from bio-based natural raw materials should be developed [22]. In developing a JCO-based NIPU, some step paths can be followed. Haniffa et al. previously examined the synthesis of JCO-based NIPU utilizing two curing agents, 1,3-diamino propane and isophorone diamine. Mechanical, thermal, solvent, and chemical resistance were all improved by combining carbonated JCO-based NIPU with carbonated alkyd resin NIPU [22]. Gogoi et al. [10] epoxidized JCO with hydrogen peroxide and formic acid mixture. The utilization of ring-opening (ROP) reaction on the epoxidation of JCO for polyol formation in PU production was investigated by Błażek et al. [24,25]. We used a novel approach to the synthesis of JCO-based NIPU in this study, which has never been published to our knowledge. To make peroxyacetic acid, we employed in situ epoxidation using hydrogen peroxide and acetic acid. The epoxidized CJO (ECJO) was then treated with carbon dioxide to produce JCO (cyclic carbonate) (CJCO). Finally, CJCO was reacted with 3-Aminopropyltriethoxysilane (APTES) and lithium chloride (LiCl) as a catalyst to create urethane JCO (UJCO). The goal of this research was to understand how catalyst loading and stirring time affected the optimum conditions of ECJO, CJCO, and UJCO.

2 Material and Methods

2.1 Materials

Jatropha curcas oil (JCO) was purchased from Lansida. Hydrogen peroxide (Merck) and glacial acetic acid (Merck) were used to convert JCO into EJCO with sulfuric acid (Merck) as a catalyst. Carbon dioxide gases and tetrabutylammonium bromide (TBAB) (Merck) were used to convert EJCO to CJCO. Lithium chloride (Sigma-Aldrich) was obtained from Sigma-Aldrich as a catalyst. 3-Aminopropyltriethoxysilane or APTES (Sigma-Aldrich) was used to produce UJCO. Other chemicals were used directly in pro analytical grade without purification.

2.2 Synthesis of EJCO

The epoxidation of JCO into EJCO was based on the previous technique of Arbain et al. [13] and Lee et al. [12] with modification. In the three-neck round bottom flask, 50 grams of JCO was introduced, followed by 26.07 mL of glacial acetic acid and 0; 0.01; 0.04; 0.08; 1.3; 2.6; and 3.9% (w/w) sulfuric acid as a catalyst. At a temperature of 10°C and 525 rpm, 88.22 mL of hydrogen peroxide was supplied dropwise to the reactor. The reactor was then heated to 60°C for 3, 4, 5, and 6 h. 1:2:9 and 1:4:9 are the mole ratios of JCO, glacial acetic acid, and hydrogen peroxide. The sample was washed with sodium chloride solution until it was neutralized in a separating funnel. A rotary evaporator was used to extract the residual solvent. Furthermore, the functional groups of the EJCO were identified using Fourier Transform Infra-Red spectroscopy (FTIR), and the oxirane and iodine values were calculated. A detail of the characterization procedure is available in the next section.

2.3 Synthesis of CJCO

The synthesis of CJCO has used the modified method of Lee et al. [12]. Fifty grams of EJCO were placed in a 150 mL three-neck round bottom flask. Then 1, 3, 6, and 9% (w/w) TBAB were added, along with a continuous supply of carbon dioxide at a rate of 0.2% per minute. For 24 and 48 h, the reactor was mechanically agitated at 900 rpm and heated to 140°C. Then CJCO was analyzed the oxirane and hydroxyl value and characterized by FTIR.

2.4 Synthesis of UJCO

The method for conversion into UJCO from CJO was modified by Lee et al. [12]. The research design of the synthesis of UJCO is shown in Table 1. 30 grams of CJCO were mixed with 6.6% LiCl relative to grams of CJCO in a 150 mL three-neck round bottom flask. Then, in a 1:1 molar ratio with CJCO, APTES was introduced to the process. The reactor was heated to 70°C for 1, 3, and 6 h while being agitated at 1200 rpm. Finally, the hydroxyl and oxirane values were analyzed and then confirmed the functional groups on the UJCO sample by FTIR.

Table 1: Experimental design of UCJO synthesis used in this work

CJCO (g)	Reaction time (h)	LiCl (%)	Mole ratio CJCO: APTES
30	1	6.6	1:1
30	3	6.6	1:1
30	6	6.6	1:1

2.5 Functional Group Identification by FTIR

The functional groups of samples were characterized by FTIR Shimadzu IR Prestige 21 (Kyoto, Japan). The sample was blended with KBr in a ratio of 1:100, and the mixture was crushed together and put on the

sample holder. The spectrum was recorded at a wavelength of 4000–450 cm^{-1} , scanning number of 40 scans, and scanning resolution of 4 cm^{-1} .

2.6 Iodine Value Analysis

Determination of iodine value followed the specifications of SNI 01-3555-1998 [26]. Briefly, 0.13 g of sample was weighed in a flask, and each 10 mL of Wijs reagent and 10 mL CCl_4 was added into the flask. 10 mL potassium iodide and 50 mL water were added to the mixture after it had been stored in a dark place for 1 h. A pale-yellow tint was achieved by titrating the mixture with sodium thiosulfate 0.1 N. 1 mL of amylum was eventually added as an indicator, and the titration was maintained until the liquid was colorless. The iodine value was calculated by using the following Eq. (1):

$$\text{iodine value} \left(\frac{\text{I}_2 \text{ g}}{100 \text{ g}} \right) = \frac{S \times N \times 12,69}{m} \quad (1)$$

where S is the volume of sodium thiosulfate for titration (mL); N is the concentration of sodium thiosulfate (N); m is sample weight (g).

2.7 Oxirane Measurement

Oxirane was analyzed according to ASTM D1652-97 [27]. In a flask, a sample of 0.3–0.5 g was weighed, and 10 mL of acetic acid glacial was added, along with a drop of crystal violet indicator. After titrating the combination with 0.1 N HBr, the oxirane value was estimated using the equation below (2):

$$\text{Oxirane value (\%)} = \frac{S \times 1,6 \times N}{m} \quad (2)$$

where S is the volume of HBr for titration (mL); N is the concentration of HBr (N); m is the weight of the sample (g).

2.8 Hydroxyl Value Determination

Hydroxyl value was determined following the method of ASTM D-4274-88 [28]. A 1 g sample was added with a 5 mL acetylation reagent (12.7 mL of acetate anhydrate glacial + 100 mL of pyridine). The mixture was refluxed for 1 h at 98°C. Moreover, 20 mL of water and 20 drops of phenolphthalein were added to the mixture. 0.5 N of NaOH was used as a titrant. Hydroxyl value was obtained by following Eq. (3):

$$\text{hydroxyl value} \left(\frac{\text{mg}}{\text{g}} \text{ sample} \right) = \frac{S \times N \times 40}{m} \quad (3)$$

where S is the volume of NaOH for titration (mL); N is the concentration of NaOH (N); m is the weight of the sample (g).

3 Results and Discussion

3.1 Synthesis of EJCO

The JCO comprises fatty acid triglycerides with long aliphatic chains, which are responsible for the coating's exceptional elasticity [15]. Most components of JCO are oleic acid and linoleic acid, with the amount of them being 34.3%–45.8% and 29.0%–44.2%, respectively [10,14]. Aside from that, it has a lower palmitoleic acid concentration [10]. These components have the potential to become materials for producing epoxy. Epoxidation through a reaction between acetic acid and hydrogen peroxide as a result, peroxyacetic acid is produced as an oxidizing agent. The mechanism of the epoxidation reaction is illustrated in Fig. 1. The double bond of JCO was oxidized by peroxyacetic acid when the reaction was ongoing. As a result, the epoxy ring was obtained. Epoxidation is attractive because it produces hydroxyl

and epoxy functionalized derivatives. Along fatty acid chains, epoxidation of unsaturated bonds occurs, resulting in a highly reactive oxirane group [29].

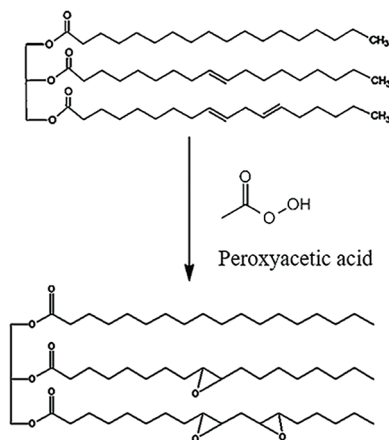


Figure 1: Illustration of the epoxidation reaction mechanism

Previously, Goud et al. [14] reported *in situ* epoxidation using a mixing of formic or acetic acid and 30% hydrogen peroxide with sulfuric acid presence in or without toluene. Because hydrogen peroxide has low solubility in oil, epoxidation is normally done with an organic peroxy acid. The oxygen carrier formic acid is hydrogen peroxide, while the oxygen donor is hydrogen peroxide [30]. This route is preferred because it uses the least amount of reactant to create the epoxidizing reagent and allows for easier preparation and handling [31]. This reaction could be influenced by catalyst, temperature, stirring speed, time of reaction, and concentration of reactant. The investigation of such variable effect on epoxidation of fatty acid from vegetable oil showed a variation in the result of its parameter [32].

3.1.1 Effect of Catalyst Loading

Amberlyst 15, enzymatic catalysts like lipase, SnCl_4 , clay, bentonite, a metal catalyst like titanium, molybdenum, tungsten, and a strong mineral acid like sulfuric acid might all be used as epoxidation catalysts [33,34]. Nonetheless, sulfuric acid is considered the most selective catalyst. Therefore, the present reaction was used considering its low cost. Acidic ion exchange resin as catalyst was reported in *in situ* epoxidations of cottonseed oil by peroxyacetic acid using hydrogen peroxide and glacial acetic acid [34,35]. This catalyst is also used in the epoxidation of soybean oil and jatropha methyl ester, as carried out by Kousaalya et al. [36] and Derahman et al. [37]. Quantitative identification for evaluating the effect of the catalyst during epoxidation processes was evaluated by measuring the iodine and oxirane value. The oxirane value is a crucial factor in preserving the structural integrity of epoxides [29]. The higher the oxirane value, the better-obtained epoxy compound as a consideration of better quality [38–40]. The epoxide ring has completely reacted in the hydroxylation reaction, releasing hydroxyl, as shown by the oxirane number [33]. The epoxide ring has completely reacted in the hydroxylation reaction, as shown by the oxirane number, creating hydroxyl.

The amount of unsaturated fatty acids in oils was determined by the iodine number. The greater iodine number accounts for the presence of more double bonds. The lower the melting point, the higher the epoxy content. The fat with a low iodine number is more resistant to degradation due to oxidation [41–43]. Fig. 2 represents the number of milligrams of iodine essential to saturate the fatty acids in 100 milligrams of oil, and the effect of catalysts to produce EJCO is indicated by iodine and oxirane value.

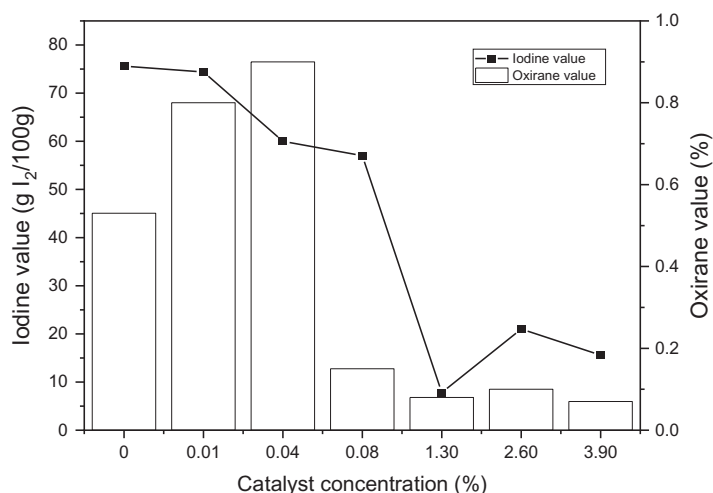


Figure 2: Effect of catalyst loading on iodine and oxirane value

Overall, the iodine value decreased with increasing the amount of catalyst, indicating the breakdown of the double bond in triglyceride JCO. The increase of catalyst concentration creates oil containing more saturated fatty acid, as represented by a lower iodine value. Rames et al. [44] previously reported that saturated fatty acids have a low iodine level, whereas unsaturated fatty acids have a high iodine concentration. Meanwhile, Folayan et al. evaluated the influence of unsaturation degree on the iodine value of three vegetable oil, where the iodine value rises as the unsaturation degree rises but falls as the chain length grows [45]. The oxirane value increased at some point, but the excessive concentration of catalyst then could decrease it. The highest oxirane value was approximately 1 at 0.04% sulfuric acid and the lowest at about 0.07%. In general, as the concentration of sulfuric acid rises, so does the value of oxirane [46]. However, it was not observed in this study. Therefore, adding a catalyst to this reaction must be carried out carefully because excess sulfuric acid addition can interfere stability of epoxy, resulting in decreasing in oxirane value. Besides that, a high concentration of sulfuric acid can degrade epoxy highly, such as 1% per hour at ambient temperature and 100% per 1–4 h at a temperature of 65–100°C [47,48]. Furthermore, Malarczyk-Matusiak et al. mentioned that it is not necessary to add a catalyst if the reaction involves peroxyacetic acid [49]. Thus, considering the study results, the reaction did not require a catalyst. It might be due to the low stability of epoxy ring formation that caused a re-opening of the epoxy ring, and then polyol compound (hydrolysis reaction) or acetone compound (acylation reaction) were produced as shown in Fig. 3. The decrease in polyol oxirane number would increase the hydroxyl value. The consumption of catalysts would be significant if the hydroxyl value was high [50].

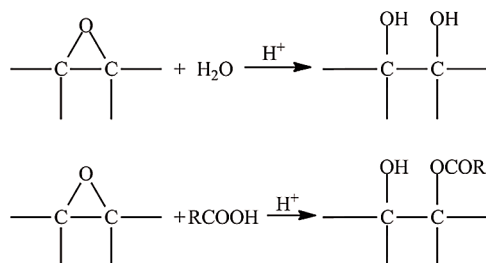


Figure 3: Hydrolysis reaction (above) and acylation reaction (below)

3.1.2 The Effect of the Mole Ratio of CH_3COOH to Ethylenic Unsaturation

Acetic acid was used as a reactant with hydrogen peroxide. The effect of CH_3COOH concentration on iodine and oxirane value has been known in which the higher mole concentration of acetic acid is obtained at higher oxirane and lower iodine values, respectively. In this condition, the reaction speed increased along with a greater amount of acetic acid, which caused the increasing frequency of collisions between involved molecules [51,52], as illustrated in Fig. 4. The graph reveals an increase of oxirane value in using acetic acid with the concentration of 4 moles on triglyceride mole without catalyst addition. The iodine value of the first ratio (1:2:9) was higher than the second ratio (1:4:9), and the oxirane value was conversely. At this term, the acetic acid also acted as a catalyst to obtain peroxyacetic acid which is required for producing epoxy rings [14]. Thus, in this epoxidation reaction, the mol ratio of glacial acetic acid and JCO of 4:1 is recommended.

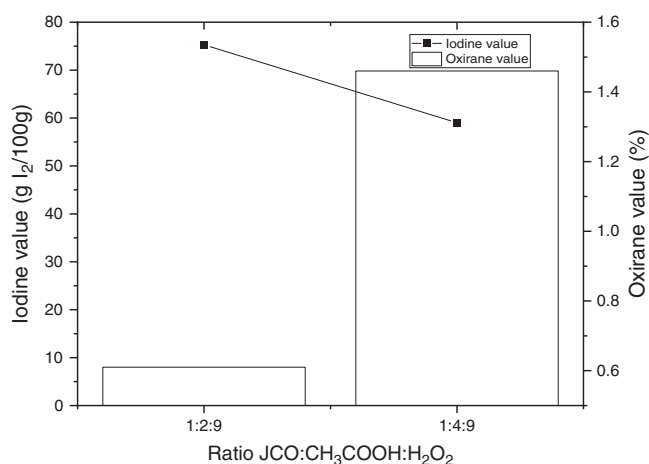


Figure 4: Effect of acetic acid concentration on iodine and oxirane value

3.1.3 Effect of Stirring Time Variation

According to Le Chatelier's principle, the stirring time did not affect the reaction equilibrium. A previous study reported that there is a positive, strong correlation (R^2 of 0.93) between reaction time with oxirane value in the epoxidation of JCO and palm oil mix (CPO) [38,39]. As shown in Fig. 5, the iodine value continues to decrease with prolonged reaction time since the double bond in triglyceride of JCO will be oxidized by peroxyacetic acid [53]. This graph means that the number of double bonds in EJCO was reduced, as has the amount of oleic acid reacted with peracetic acid. The epoxides were then assessed. The oxirane number denotes the exact value of the product [54]. The oxirane value was increased by increasing reaction time, and the value decreased again at a certain time.

The oxirane value increased significantly from 0% to 1.46% during the first 5 h and then decreased steadily until the end of time. The addition of time did not contribute effectively to transforming glacial acetic acid to peroxyacetic acid, although it would decompose again to form acetic acid since the reaction of production of peroxyacetic acid is reversible. This reaction for 5 h is suggested based on oxirane value. The different pattern of iodine value and oxirane value by reaction time of technical grade oleic acid epoxidation was also reported before by Dyah Retno et al. [54].

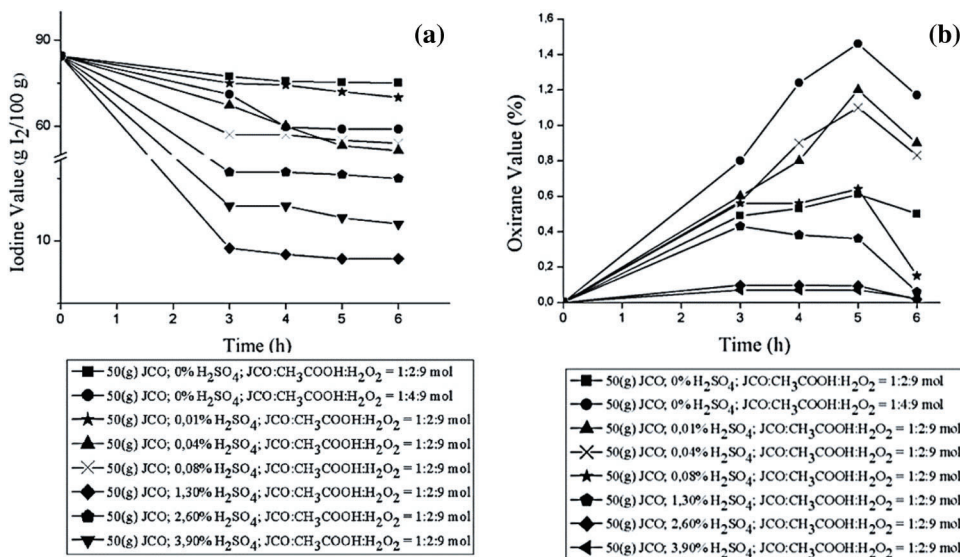


Figure 5: Effect of stirring time on (a) Iodine value and (b) Oxirane value

3.2 Synthesis of CJCO

3.2.1 Effect of Catalyst Loading

The use of cyclic carbonates and amines in the synthesis of NIPU is an appealing method in this reaction. The CJCO synthesis method is carried out by substituting CO₂ gas on the EJCO in the percent of the TBAB catalyst. Several catalysts have been known in the synthesis of carbonate cyclic compounds from epoxide compounds. Under supercritical conditions, epoxidized sucrose soyate can be converted to carbonate sucrose soyate using this process [55]. As a result, this approach was chosen for the current investigation. TBAB was selected to be investigated the effect of catalysts during synthesizing CJCO from EJCO. TBAB has been identified as the best homogenous catalyst for converting epoxy ring into cyclic carbonate at a high temperature with conversion >90% [22,56,57]. TBAB can catalyze carbon dioxide gas bonding on epoxide compound in pressure of 1 atm. Catalyst, temperature, reaction time, and pressure are identified as the main factors affected by the synthesis steps of cyclic carbonate [56,58]. The optimum temperature of cyclic carbonate is 140°C, and this value was also used in this study [59].

At high temperatures, TBAB can degrade dangerous and volatile chemicals such as hydrogen bromide, which is highly reactive with epoxy groups [22]. As an activator, TBAB will break to open the epoxy, causing an attack of the bromide nucleophile, followed by carbon dioxide will activate the ring, and as a result, cyclic carbonate is formed as illustrated in Fig. 6. Consequently, the oxirane value was decreased sharply from 1.46 to 0 at 6% and 9% concentrations of the catalyst indicating the formation of cyclic carbonate from EJCO (Fig. 7). It can be affected by the bonding of carbon dioxide gas becoming more effective with increasing in catalyst amount. During the reaction, TBAB, as an activator catalyst, will open the ring of the epoxy compound due to the nucleophilic attack of the bromide ion, which then CO₂ (electrophilic attack on the oxygen atom) will be fixed on the ring and close again into a cyclic carbonate ring accompanied by the re-release of TBAB.

The hydroxyl value decreased with the increase in catalyst amount, as shown in Fig. 7. Zhang et al. [56] and Mazo et al. [60] identified a link between the number of catalysts employed and the creation of cyclic carbonate compounds, which shows that the number of catalysts used enhances the conversion of epoxy compounds to cyclic carbonate compounds. In the study of Mazo et al. [60], using the TBAB in the range of 3% to 5% (mole), the reaction kinetics tended to increase from 0.1 to 0.9, respectively. Zhang

et al. [56] used the amount of catalyst in the range of 0.01% to 0.065% (mole/epoxy), in which at a catalyst amount of 0.04%, the conversion to cyclic carbonate compounds was up to 99.9%.

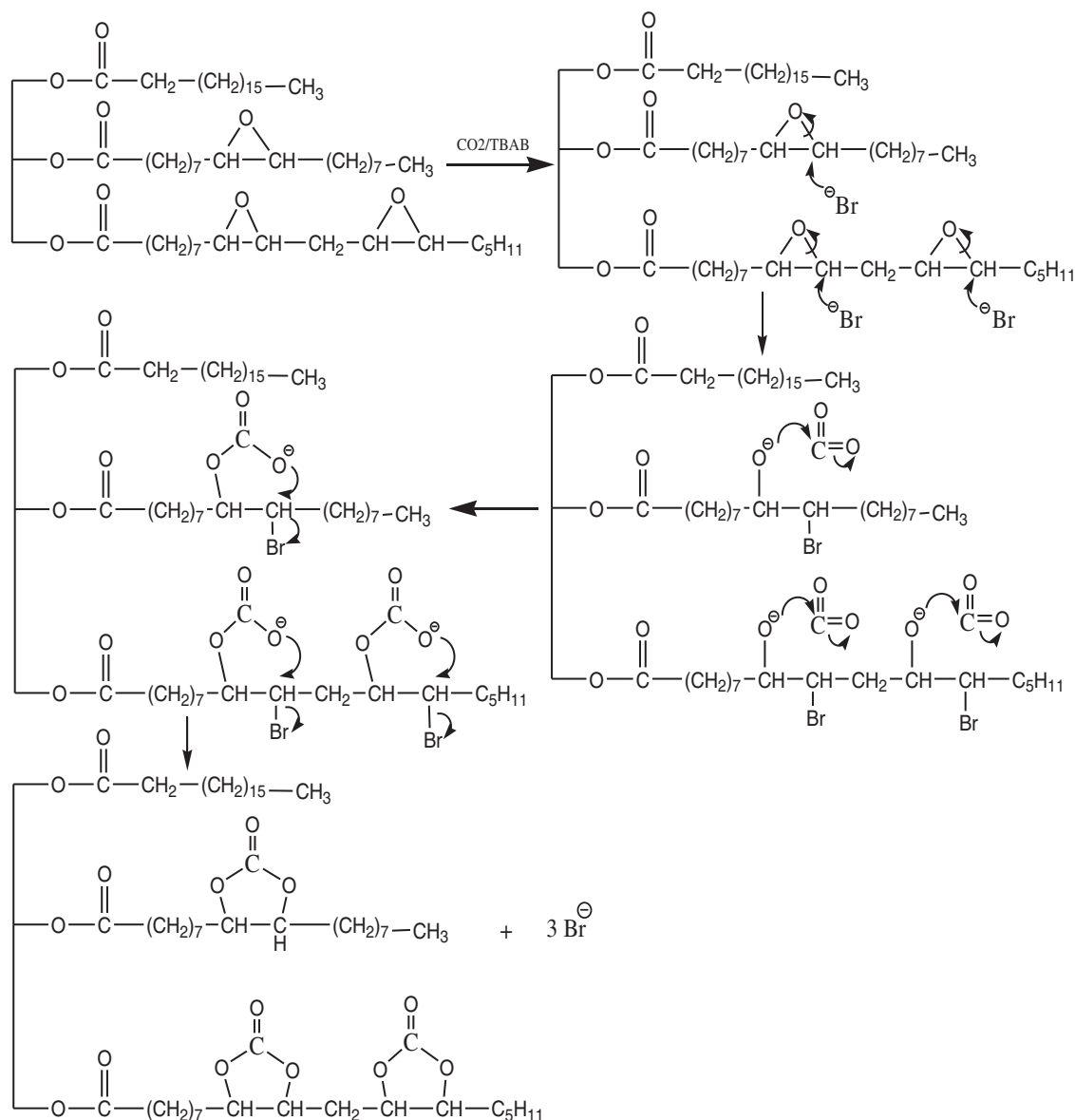


Figure 6: Synthesis mechanism of cyclic carbonate of CCJO

3.2.2 Effect of Stirring Time

The stirring time is a variable in cyclic carbonates reaction observed in this study by assessing the oxirane value and hydroxyl value. As presented in Fig. 8, the equilibrium reactions occur when the sample is reacted for 48 h. The longer the reaction period, the more likely the reactants would collide, increasing the likelihood of side reactions. It can cause the oxirane ring to open, resulting in a reduction in the oxirane value in the epoxy [38,39].

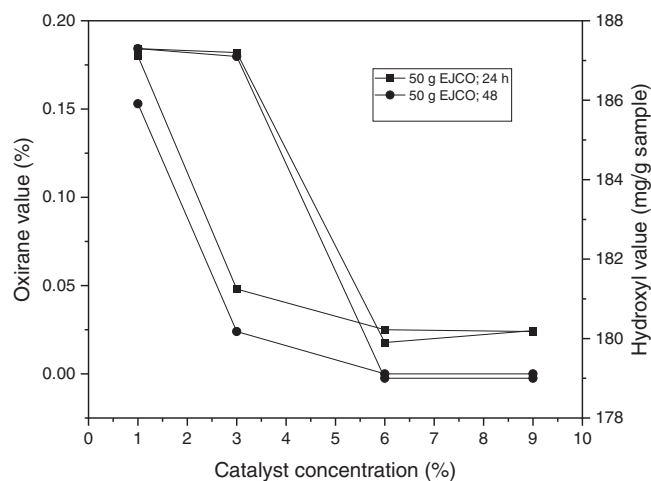


Figure 7: Effect of catalyst loading on oxirane value and hydroxyl value

The highest oxirane value was up to 1.4% in the first period, and the lowest oxirane value was almost 0% at the end of the period, which indicates that the conversion yield of EJCO to CJCO is almost complete, about 99.9%. As previously reported by Haniffa et al. [22], this conversion was carried out at a temperature of 140°C within the temperature range of cyclic carbonate of JCO. At a similar temperature, our study produced a higher conversion yield. As previously indicated, the opening of the oxirane group to form a hydroxyl group is required to produce polyol from epoxidized vegetable oils [61] thus, the hydroxyl value was determined. The average distribution of hydroxyl groups contained in triglycerides [62], which will impact the characteristics of the PU, is referred to as the hydroxyl value of polyol. Even though the previous study reported that there is a positive correlation (R^2 of 0.98) between the hydroxyl value obtained with reaction time [38,39], the hydroxyl value is almost stable at all times, as illustrated in Fig. 8. These hydroxyl values are higher than the hydroxyl number of a polyol as PU film from JCO by ROP, about 81.28 mg KOH/g and 117.43 mg KOH/g [63]. Thus, the addition of 6% TBAB with 48 reaction time is preferred used in the synthesis of CJCO from EJCO.

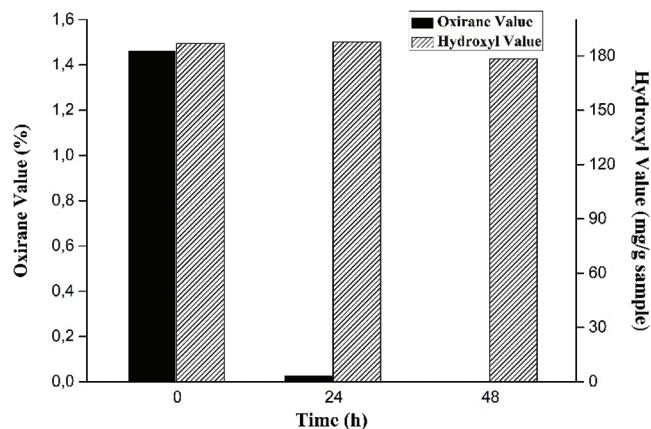


Figure 8: Effect of stirring time on oxirane value and hydroxyl value

3.3 Synthesis of UJCO

The reaction for producing UJCO occurs between CJCO with APTES, which has the excellent activity of amine with cyclic carbonate; thus, the urethane and secondary hydroxyl groups could be obtained. Lewis catalyst additions, such as LiCl, can influence reaction speed by activating the cyclic carbonate without deactivating the amine. The weak Lewis can increase electrophilic or nucleophilic amine. Thus, this addition in cyclic carbonate is suitable for producing high PU products [64]. In addition, the presence of silane in APTES can be bonded to each other to produce a siloxane (-Si-O-Si-) bond resulting in more hydrophobic PU [65]. The reaction mechanism of UJCO formation is illustrated in Fig. 9. The effect of temperature can indeed increase the reaction rate, but at higher temperatures, it can cause a reaction between amines and esters and have amides as side products [66].

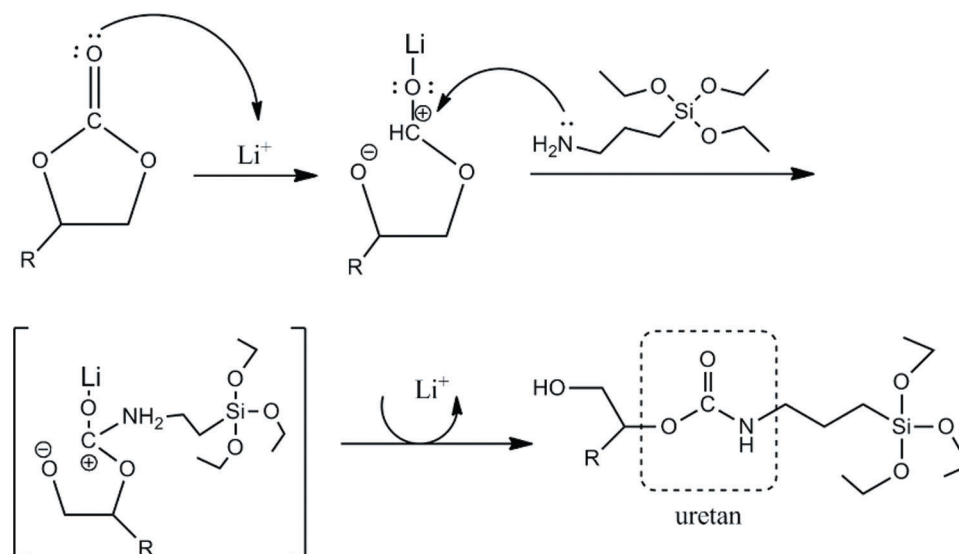


Figure 9: Reaction mechanism of synthesis of urethane

3.3.1 Effect of Stirring Time Variation

The hydroxyl value was calculated because the cyclic carbonate reacts with amine producing urethane and hydroxyl groups. As the reaction time increases, the hydroxyl value of UJCO obtained increases. When cyclic carbonates react with amines, hydroxyl groups and urethane are formed [55]. The additional time could increase the hydroxyl value, although the yield drops back at a certain time, which indicates the reaction had passed its equilibrium. The initial hydroxyl value was 179.92 mg/g sample, followed by a moderate increase to 234 mg/g sample during the 3-h reaction time. This hydroxyl value then decreased with proloner time (6 h), as illustrated in Fig. 10. It is suggested that reaction equilibrium occurred during a reaction time of 5 h to result in the formation of amides and decreased hydroxyl number. The increase in hydroxyl number indicated the opening cyclic carbonate ring of CJCO to react with amine from APTES, as presented in Fig. 9.

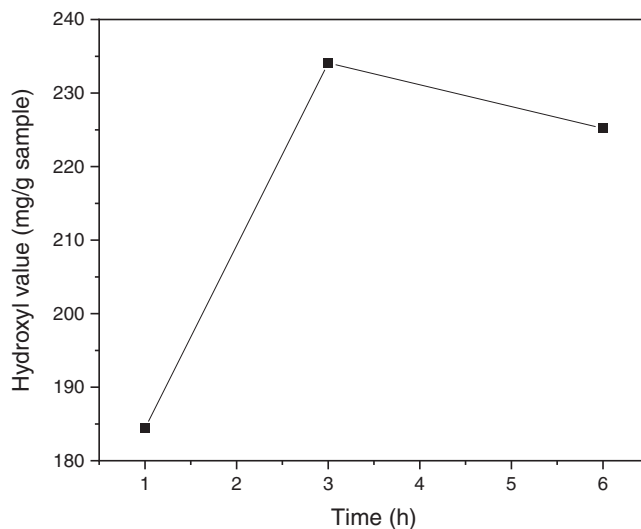


Figure 10: Effect of reaction time on hydroxyl value

3.4 Characterization of Functional Groups by FTIR

FTIR spectroscopy was used to study the functional groups of JCO, EJCO, CJCO, and UJCO, as shown in Fig. 11. The respective peaks of JCO were identified at 3003 cm^{-1} (assigned to $-\text{CH}=\text{CH}-$) and 1739 cm^{-1} ($\text{C}=\text{O}$ stretching vibration) which indicated the availability of ester (Fig. 11a). In addition, the double bond of JCO disappeared when the EJCO was obtained, and the peaks of the epoxy group ($\text{C}-\text{O}-\text{C}$) were observed at 848 cm^{-1} , as shown in Fig. 11b. Derawi et al. [67] reported that the epoxy group from the epoxidation reaction was obtained at the wavenumber of 844 cm^{-1} .

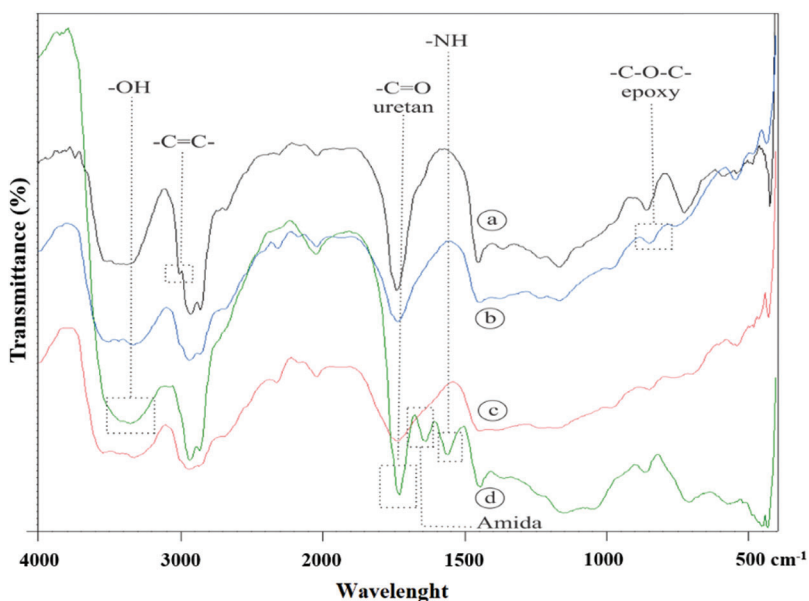


Figure 11: Comparison of the FTIR of (a) JCO; (b) EJCO; (c) CJCO; (d) UJCO

The respective peaks of CJCO are shown in Fig. 11c. Nevertheless, the peak of cyclic carbonate (carbonate cyclic carbonyl $\text{C}=\text{O}$) was not identified as a result of the formation of CJCO depending on

the decrease of oxirane value. Previously, Javni et al. [66] identified this functional group resulting from the synthesis of carbonate cyclic of soybean oil at 1803 cm^{-1} . FTIR was also used to confirm the functional groups of UJCO, as shown in Fig. 11d, with the carbonyl urethane peak at 1732 cm^{-1} , the hydroxyl peak at 3348 cm^{-1} , and the amine peak at 1562 cm^{-1} . These results are by the findings, reported by Tamami et al. [68]. The occurrence of absorption at 1639.49 cm^{-1} suggested the presence of an amide compound generated during the urethane synthesis reaction between the ester and an amine. Based on the identification, it was proven that urethane compounds had been formed in UJCO.

3.5 Prospective Application of UJCO as an Eco-Friendly NIPU for Wood Composites

Due to the abundance of Jatropha plantations around the world, the use of Jatropha oil as a renewable feedstock in the manufacturing of polyols and the corresponding PU has a bright future. The availability of these materials is practically unlimited as it is expected to have 12.8 million Jatropha being planted globally. It was estimated from the year 2008 that there are also missing hectares (12.8 million) [69,70]. Furthermore, crude oil price fluctuations significantly impact the price of traditional PU. Green PU from a different source could be a partial solution for price stability. These renewable raw resources may not be able to compete with the products of the petrochemical sector at the moment, but this will change as the supply of oil diminishes [71]. Besides, the isocyanate is highly critical in PU manufacturing since it is associated with serious health hazards, such as irritation and sensitization. Therefore, developing a reaction pathway to either minimize or eliminate toxic isocyanate in PU production has gained increased research interest [72], especially in the use of alternative natural raw materials.

In this study, non-edible vegetable oil (JCO) was converted to monomer urethane of UJCO by reacting carbonated JCO with diamines, demonstrating its potential to be used as an eco-friendly monomer urethane due to the high content of hydroxyl value and the presence of carbonyl urethane peak. Saalah et al. [73] reported the synthesis of waterborne PU from JCO with a range of hydroxyl values of 138 to 217 mgKOH/g and characterized by good pendulum hardness, water repellence, and thermal stability. Our study obtained a slightly higher hydroxyl value of 234 mgNaOH/g. It is predicted that the monomer urethane would have similar chemical properties as the one reported by Saalah et al. [73]. Hence the synthesized monomer urethane could be suitable for coating and decorative applications. Previously, it was stated that the suitable PU for decorative and wood coatings would be provided with the high OH value of waterborne PU because it increased dispersion stability and decreased the particle size. In another research, high hydroxyl of waterborne PU in an application of clay nanocomposites showed good compatibility and distributed equally throughout the polymer matrix [74]. Meanwhile, Aung et al. [75] compared the performance of PU composites from JCO (PU-JCO) based and Palm oil (PU-PO)-based for the synthesis of wood adhesives, and the result showed that the chemical characteristics and shear strength of composites bonded with PU-JCO adhesives were better than PU-PO in response to alkali, acid, and hot water [75]. In addition to wood adhesive applications, PU-JCO could be a feasible option for the paint coating material. In their study, Harjono et al. [63] reported that PU film made from epoxidized JCO exhibited similar gloss, hardness, and adhesion quality as the PU film synthesized from commercial polyol.

Vegetable oil-based alkyd resins have many broad applications in wood composite products such as surface coating and adhesive. However, these resins have a few significant disadvantages, including low heat stability, limited hardness, poor mechanical strength, and a long curing period. These shortcomings can be alleviated by mixing the alkyd resins with other epoxidized resins. Gogoi et al. [10] mixed JCO-based alkyd resins with epoxidized JCO to improve the curing time, hardness, tensile strength, elongation at break, gloss, and adhesion where the results were compared with alkyd resin without mixing. The result showed that mixture one had a shorter curing time, higher hardness, improved tensile strength, elongation break, gloss, and excellent adhesion as well. Besides, the thermal stability notably

increased as a result of the improved density of cross-linking and interaction of H-bonding in the polar functional [10]. Another research by Saravari and Praditvatanakit reported adhesion properties mixture of urethane JCO-based alkyd/Castor oil. Even though the urethane JCO-based alkyd/Castor oil had lower hardness, molecular weight, and density compared to commercial and conventional urethane, it demonstrated good adhesion and resistance to acid and water. To note, the blending of urethane JCO-based alkyd and epoxidized vegetable oil/virgin has potential applications as a wood adhesive [76].

Amri et al. reviewed the performance of PU JCO based on other vegetable oil in the nanocomposite's PU/cellulose nanocrystal. According to the report, there will be an increased scientific and industrial interest related to the enhanced valorization of these materials in a wide range of commercial applications, including wood adhesives [77]. Nanocellulose could be used as a reinforcing component in plant-oil-based PU, according to a study by SaifulAzry et al. [78]. The Young's modulus and tensile strength of the JCO-PU-based nanocomposite have improved significantly due to nanocellulose incorporation. Markedly, it is expected that the PU based on JCO and their derivatives will gain considerable industrial interest and increased utilization in wood composite applications due to their favorable properties. In terms of environmental impact, polyols based on vegetable oils or other bio-based oils have also been identified as posing lesser environmental impacts [5,79–84]. Fridrihsone et al. [85] found that the utilization of rapeseed oil as a green feedstock for the production of polyol leads to lower non-renewable energy and water consumption and lower GHG emissions compared to that of the synthetic polyol. The study found that producing bio-polyol from vegetable oils for PU synthesis has environmental benefits. However, more research is needed to address the disadvantages of vegetable oils.

4 Conclusions

In this study, the urethane monomer was synthesized successfully from *Jatropha curcas* oil, although the conversion of hydroxyl value was not 100%. It can be confirmed by the presence of functional groups at 1732.08, 1562.34, and 3348.42 cm^{-1} in FTIR spectra, indicating the functional groups of C=O (urethane carbonyl), –NH, and –OH, respectively. It was concluded that the optimal condition for the synthesis of EJCO is 5 h with a mole ratio of acetic acid to JCO of 4:1 without the addition of sulfuric acid as a catalyst. The time required for transforming EJCO to CJCO was determined to be 48 h with the addition of 6% TBAB as a catalyst.

Acknowledgement: This study was financially supported by DIPA Mandiri LIPI, Indonesia. This research was also supported by Project No. НИС-Б-1145/04.2021, “Development, Properties, and Application of Eco-Friendly Wood-Based Composites,” carried out at the University of Forestry, Sofia, Bulgaria, and by the Slovak Research and Development Agency under Contracts Nos. APVV-18-0378, APVV-19-0269, and APPV-20-0004.

Funding Statement: The authors received no specific funding for this study.

Conflicts of Interest: The authors declare that they have no conflicts of interest to report regarding the present study.

References

1. Aristri, M. A., Lubis, M. A. R., Yadav, S. M., Antov, P., Papadopoulos, A. N. et al. (2021). Recent developments in lignin-and tannin-based non-isocyanate polyurethane resins for wood adhesives—A review. *Applied Sciences*, 11(9), 4242. DOI 10.3390/app11094242.
2. Eling, B., Tomović, Ž., Schädler, V. (2020). Current and future trends in polyurethanes: An industrial perspective. *Macromolecular Chemistry and Physics*, 221(14), 2000114. DOI 10.1002/macp.202000114.

3. Ghasemlou, M., Daver, F., Ivanova, E. P., Adhikari, B. (2019). Polyurethanes from seed oil-based polyols: A review of synthesis, mechanical and thermal properties. *Industrial Crops and Products*, 142(115), 111841. DOI 10.1016/j.indcrop.2019.111841.
4. Ionescu, M., Radojčić, D., Wan, X., Shrestha, M. L., Petrović, Z. S. et al. (2016). Highly functional polyols from castor oil for rigid polyurethanes. *European Polymer Journal*, 84(3), 736–749. DOI 10.1016/j.eurpolymj.2016.06.006.
5. Sawpan, M. A. (2018). Polyurethanes from vegetable oils and applications: A review. *Journal of Polymer Research*, 25(8), 184. DOI 10.1007/s10965-018-1578-3.
6. Sahoo, S., Mohanty, S., Nayak, S. K. (2018). Biobased polyurethane adhesive over petroleum based adhesive: Use of renewable resource. *Journal of Macromolecular Science, Part A*, 55(1), 36–48. DOI 10.1080/10601325.2017.1387486.
7. Akindoyo, J. O., Beg, M. D. H., Ghazali, S., Islam, M. R., Jeyaratnam, N. et al. (2016). Polyurethane types, synthesis and applications—A review. *RSC Advances*, 6(115), 114453–114482. DOI 10.1039/C6RA14525F.
8. Golling, F. E., Pires, R., Hecking, A., Weikard, J., Richter, F. et al. (2019). Polyurethanes for coatings and adhesives—chemistry and applications. *Polymer International*, 68(5), 848–855. DOI 10.1002/pi.5665.
9. Alam, M., Alandis, N. M., Zafar, F., Sharmin, E., Al-Mohammadi, Y. M. (2018). Polyurethane-TiO₂ nanocomposite coatings from sunflower-oil-based amide diol as soft segment. *Journal of Macromolecular Science, Part A*, 55(10), 698–708. DOI 10.1080/10601325.2018.1526638.
10. Gogoi, P., Boruah, M. S. S., Dolui, S. K. (2015). Blends of epoxidized alkyd resins based on jatropha oil and the epoxidized oil cured with aqueous citric acid solution: A green technology approach. *ACS Sustainable Chemistry & Engineering*, 3(2), 261–268. DOI 10.1021/sc500627u.
11. Coureau, E., Fontana, L., Lamouroux, C., Pélissier, C., Charbotel, B. (2021). Is isocyanate exposure and occupational asthma still a major occupational health concern? Systematic literature review. *International Journal Environment Resource Public Health*, 18(24), 13181. DOI 10.3390/ijerph182413181.
12. Lee, A., Deng, Y. (2015). Green polyurethane from lignin and soybean oil through non-isocyanate reactions. *European Polymer Journal*, 63(1–2), 67–73. DOI 10.1016/j.eurpolymj.2014.11.023.
13. Arbain, N., Salimon, J., Salih, N., Abdo, W. (2021). Optimization for epoxidation of Malaysian *Jatropha curcas* oil based trimethylolpropane ester biolubricant. *Applied Science and Engineering Progress*, 15(3), 5552. DOI 10.14416/j.asep.2021.10.009.
14. Goud, V. V., Dinda, S., Patwardhan, A. V., Pradhan, N. C. (2010). Epoxidation of *Jatropha (Jatropha curcas)* oil by peroxyacids. *Asia-Pacific Journal of Chemical Engineering*, 5(2), 346–354. DOI 10.1002/apj.285.
15. Pathak, R., Kathalewar, M., Wazarkar, K., Sabnis, A. (2015). Non-isocyanate polyurethane (NIPU) from tris-2-hydroxy ethyl isocyanurate modified fatty acid for coating applications. *Progress in Organic Coatings*, 89(899), 160–169. DOI 10.1016/j.porgcoat.2015.08.015.
16. Martínez Ponce, A., Mijangos, G., Romero, I., Hernández Altamirano, R., Mena-Cervantes, V. (2019). *In-situ* transesterification of *Jatropha curcas* L. seeds using homogeneous and heterogeneous basic catalysts. *Fuel*, 235, 277–287. DOI 10.1016/j.fuel.2018.07.082.
17. Naji, S. Z., Tye, C. T., Abd, A. A. (2021). State of the art of vegetable oil transformation into biofuels using catalytic cracking technology: Recent trends and future perspectives. *Process Biochemistry*, 109(6), 148–168. DOI 10.1016/j.procbio.2021.06.020.
18. Singh, D., Sharma, D., Soni, S. L., Inda, C. S., Sharma, S. et al. (2021). A comprehensive review of physicochemical properties, production process, performance and emissions characteristics of 2nd generation biodiesel feedstock: *Jatropha curcas*. *Fuel*, 285, 119110. DOI 10.1016/j.fuel.2020.119110.
19. Riayatsyah, T. M. I., Sebayang, A. H., Silitonga, A. S., Padli, Y., Fattah, I. M. R. et al. (2022). Current progress of *Jatropha curcas* commoditisation as biodiesel feedstock: A comprehensive review. *Frontiers in Energy Research*, 9, 815416. DOI 10.3389/fenrg.2021.815416.
20. Ewunie, G. A., Morken, J., Lekang, O. I., Yigezu, Z. D. (2021). Factors affecting the potential of *Jatropha curcas* for sustainable biodiesel production: A critical review. *Renewable and Sustainable Energy Reviews*, 137(4), 110500. DOI 10.1016/j.rser.2020.110500.

21. Das, A. K., Chavan, A. S., Shill, D. C., Chatterjee, S. (2021). Jatropha curcas oil for distribution transformer—A comparative review. *Sustainable Energy Technologies and Assessments*, 46(6), 101259. DOI 10.1016/j.seta.2021.101259.
22. Haniffa, M. A. C. M., Ching, Y. C., Chuah, C. H., Kuan, Y. C., Liu, D. S. et al. (2017). Synthesis, Characterization and the solvent effects on interfacial phenomena of *Jatropha curcas* oil based non-isocyanate polyurethane. *Polymers*, 9(5), 162.
23. Dugala, N. S., Goindi, G. S., Sharma, A. (2021). Evaluation of physicochemical characteristics of Mahua (*Madhuca indica*) and Jatropha (*Jatropha curcas*) dual biodiesel blends with diesel. *Journal of King Saud University-Engineering Sciences*, 33(6), 424–436.
24. Daniel, L., Ardiyanti, A. R., Schuur, B., Manurung, R., Broekhuis, A. A. et al. (2011). Synthesis and properties of highly branched *Jatropha curcas* L. oil derivatives. *European Journal of Lipid Science and Technology*, 113, 18–30.
25. Błażek, K., Beneš, H., Walterová, Z., Abbrent, S., Eceiza, A. et al. (2021). Synthesis and structural characterization of bio-based bis(cyclic carbonate)s for the preparation of non-isocyanate polyurethanes. *Polymer Chemistry*, 12(11), 1643–1652. DOI 10.1039/d0py01576h.
26. Indonesia, NSAO (1999). *SNI 01-3555-1998-Cara Uji Minyak dan Lemak*. BSN. Indonesia.
27. ASTM, A. I. (1997). *ASTM D1652-97-Standard Test Methods for Epoxy Content of Epoxy Resins*. Pennsylvania: ASTM. DOI 10.1520/D1652-97.
28. ASTM, A. I. (1988). *ASTM D-4274-88-Determination of Hydroxyl Numbers of Polyols*. Pennsylvania: ASTM. DOI 10.1520/D4274-21.
29. Paul, A. K., Borugadda, V. B., Goud, V. V. (2021). *In-situ* epoxidation of waste cooking oil and its methyl esters for lubricant applications: Characterization and rheology. *Lubricants*, 9(3), 27.
30. Jalil, M. J., Yamin, A. F. M., Zaini, M. S. M., Ariff, M. A. M., Chang, S. H. et al. (2019). Synthesis of epoxidized oleic acid-based palm oil by peracid mechanism. *IOP Conference Series: Materials Science and Engineering*, 214st ECS Meeting, 551, 1–5. DOI 10.1088/1757-899x/551/1/012120.
31. Mohd Nor, N., Salih, N., Salimon, J. (2021). Chemically modified *Jatropha curcas* oil for biolubricant applications. *Hemijaska Industrija*, 75(2), 117–128.
32. Jalil, M. J., Azmi, I. S., Hadi, A., Yamin, A. F. M. (2022). *In situ* hydrolysis of epoxidized oleic acid by catalytic epoxidation-peracids mechanism. *Journal of Polymer Research*, 29(3), 102. DOI 10.1007/s10965-022-02944-4.
33. Wai, P. T., Jiang, P., Shen, Y., Zhang, P., Gu, Q. et al. (2019). Catalytic developments in the epoxidation of vegetable oils and the analysis methods of epoxidized products. *RSC Advances*, 9(65), 38119–38136. DOI 10.1039/C9RA05943A.
34. Lewandowski, G., Musik, M., Malarczyk-Matusiak, K., Sałaciński, Ł., Milchert, E. (2019). Epoxidation of vegetable oils, unsaturated fatty acids and fatty acid esters: A review. *Mini-Reviews in Organic Chemistry*, 17(4), 412–422. DOI 10.2174/1570193X16666190430154319.
35. Dinda, S., Goud, V., Patwardhan, A., Pradhan, N. (2011). Selective epoxidation of natural triglycerides using acidic ion exchange resin as catalyst. *Asia-Pacific Journal of Chemical Engineering*, 6(6), 870–878. DOI 10.1002/apj.466.
36. Kousaalya, A. B., Beyene, S. D., Ayalew, B., Pilla, S. (2019). Epoxidation kinetics of high-linolenic triglyceride catalyzed by solid acidic-ion exchange resin. *Scientific Reports*, 9(1), 8987. DOI 10.1038/s41598-019-45458-8.
37. Derahman, A., Abidin, Z. Z., Cardona, F., Biak, D. R. A., Tahir, P. M. et al. (2019). Epoxidation of jatropha methyl esters via acidic ion exchange resin: Optimization and characterization. *Brazilian Journal of Chemical Engineering*, 36(2), 959–968. DOI 10.1590/0104-6632.20190362s20180326.
38. Syamsudin, A. (2012). Pengaruh waktu reaksi terhadap bilangan hidroksil pada pembentukan polyol dari epoksidasi CPO dan curcas oil. *Konversi*, 1(1), 15–24. DOI 10.24853/konversi.1.1.%25p.
39. Lye, Y. N., Salih, N., Salimon, J. (2021). Optimization of partial epoxidation on *Jatropha curcas* oil based methyl linoleate using urea-hydrogen peroxide and methyltrioxorhenium catalyst. *Applied Science and Engineering Progress*, 14(1), 89–99.

40. Hasnan, N. H. A., Yaakob, N., Abu Kassim, M. N., Mohd Noh, U. A. (2020). Significance of oxirane rings in epoxidized palm oil and effects on the coating performance: Comparison between epoxidized unripe palm oil and epoxidized used cooking oil towards adhesion performance. *Indonesian Journal of Chemistry*, 20(4), 858–869. DOI 10.22146/ijc.46619.
41. Gan, L. H., Goh, S. H., Ooi, K. S. (1992). Kinetic studies of epoxidation and oxirane cleavage of palm olein methyl esters. *Journal of the American Oil Chemists' Society*, 69(4), 347–351. DOI 10.1007/BF02636065.
42. Barradas Filho, A. O., Barros, A. K. D., Labidi, S., Viegas, I. M. A., Marques, D. B. et al. (2015). Application of artificial neural networks to predict viscosity, iodine value and induction period of biodiesel focused on the study of oxidative stability. *Fuel*, 145(1), 127–135. DOI 10.1016/j.fuel.2014.12.016.
43. Soares, S., Rocha, F. (2018). Fast spectrophotometric determination of iodine value in biodiesel and vegetable oils. *Journal of the Brazilian Chemical Society*, 29(8), 1701–1706. DOI 10.21577/0103-5053.20180044.
44. Ramesh, C. G., Gulab, K. (1994). Determination of iodine numbers of edible oils. *Biomedical Education*, 22(1), 47.
45. Folayan, A. J., Anawe, P. A. L., Aladejare, A. E., Ayeni, A. O. (2019). Experimental investigation of the effect of fatty acids configuration, chain length, branching and degree of unsaturation on biodiesel fuel properties obtained from lauric oils, high-oleic and high-linoleic vegetable oil biomass. *Energy Reports*, 5, 793–806. DOI 10.1016/j.egy.2019.06.013.
46. Sinaga, M. S., Simanjuntak, J. F., Winda, O. (2019). Effect of reaction time and catalyst concentration on making of epoxy compounds using sulphuric acid catalyst based on crystallized palm fatty acid distillate. *IOP Conference Series: Materials Science and Engineering*, 505(1), 012117. DOI 10.1088/1757-899X/505/1/012117.
47. Sinaga, M. (2010). Pengaruh katalis H₂SO₄ pada reaksi epoksidasi metil ester PFAD (Palm Fatty Acid Distillate). *Journal Teknologi Proses*, 6(1), 70–74.
48. Mekonnen, Y. (2021). Epoxidation of podocarpus falcatus oil by sulphuric acid catalyst: Process optimization and physio-chemical characterization. *American Journal of Chemical Engineering*, 9(4), 84.
49. Malarczyk-Matusiak, K., Milchert, E. (2018). Optimization of selective epoxidation of canola oil with *in situ* generated peracetic acid. *Journal of Advanced Oxidation Technologies*, 21(1), 73–83. DOI 10.26802/jaots.2017.0047.
50. Firdaus, F. E. (2014). The selection reaction of homogeneous catalyst in soy-epoxide hydroxylation. *Journal of Physics: Conference Series*, 495, 12013.
51. Okieimen, F. E., Bakare, O. I., Okieimen, C. O. (2002). Studies on the epoxidation of rubber seed oil. *Industrial Crops and Products*, 15(2), 139–144.
52. Neswati, Nazir, N. (2021). Combination of temperature and time in epoxidation for producing epoxidized palm oil as source of bio polyol. *IOP Conference Series: Earth and Environmental Science, International Conference on Sustainable Agriculture and Biosystem*, 757(1), 012069. DOI 10.1088/1755-1315/757/1/012069.
53. Elda, M., Selviany, N., Fajrin, D. (2016). Pengaruh temperatur dan waktu pada pembuatan plastisizer dengan reaksi epoksidasi minyak limbah ikan patin. *Jurnal Teknik Kimia*, 21(2), 40–44.
54. Panut, M., Rochmadi, Arief, Dyah Retno, S., Panut, M. et al. (2019). Pseudo-homogeneous kinetic evaluation for in-situ epoxidation of oleic acid. *IOP Conference Series: Materials Science and Engineering, 26th Regional Symposium on Chemical Engineering*, 1–6. DOI 10.1088/1757-899X/778/1/012052.
55. Yu, A. Z., Setien, R. A., Sahouani, J. M., Docken, J., Webster, D. C. (2019). Catalyzed non-isocyanate polyurethane (NIPU) coatings from bio-based poly(cyclic carbonates). *Journal of Coatings Technology and Research*, 16(1), 41–57. DOI 10.1007/s11998-018-0135-7.
56. Zhang, L., Luo, Y., Hou, Z., He, Z., Eli, W. (2014). Synthesis of carbonated cotton seed oil and its application as lubricating base oil. *Journal of the American Oil Chemists' Society*, 91(1), 143–150. DOI 10.1007/s11746-013-2358-1.
57. Nakibuule, F., Nyanzi, S. A., Oshchapovsky, I., Wendt, O. F., Tebandeke, E. (2020). Synthesis of cyclic carbonates from epoxides and carbon dioxide catalyzed by talc and other phyllosilicates. *BMC Chemistry*, 14(1), 61. DOI 10.1186/s13065-020-00713-2.

58. Rollin, P., Soares, L. K., Barcellos, A. M., Araujo, D. R., Lenardão, E. J. et al. (2021). Five-membered cyclic carbonates: Versatility for applications in organic synthesis, pharmaceutical, and materials sciences. *Applied Sciences*, 11(11), 5024. DOI 10.3390/app11115024.
59. Rokicki, G., Parzuchowski, P. G. (2012). ROP of cyclic carbonates and ROP of macrocycles. *Polymer Science: A Comprehensive Reference*, 10(4), 247–308.
60. Mazo, P., Rios, L. (2013). Carbonation of epoxidized soybean oil improved by the addition of water. *Journal of the American Oil Chemists' Society*, 90(5), 725–730. DOI 10.1007/s11746-013-2214-3.
61. Saalah, S., Abdullah, L. C., Aung, M. M., Biak, D. R., Basri, M. et al. (2017). Physicochemical properties of jatropha oil-based polyol produced by a two steps method. *Molecules*, 22(4), 551. DOI 10.3390/molecules22040551.
62. Lu, Y., Larock, R. C. (2008). Soybean-oil-based waterborne polyurethane dispersions: Effects of polyol functionality and hard segment content on properties. *Biomacromolecules*, 9(11), 3332–3340. DOI 10.1021/bm801030g.
63. Harjono, Purwatiningsih, S., Zainal Alim, M. U. (2012). Synthesis and application of Jatropha oil based polyurethane as paint coating material. *Makara Journal of Science*, 16(2), 134–140.
64. Lee, A. (2014). *Synthesis of polyurethane from one hundred percent sustainable natural materials through non-isocyanate reactions (Master Thesis)*. Georgia Institute of Technology, Georgia.
65. Lyu, J., Xu, K., Zhang, N., Lu, C., Zhang, Q. et al. (2019). *In situ* incorporation of diamino silane group into waterborne polyurethane for enhancing surface hydrophobicity of coating. *Molecules*, 24(9), 1667. DOI 10.3390/molecules24091667.
66. Javni, I., Hong, D. P., Petrović, Z. S. (2008). Soy-based polyurethanes by nonisocyanate route. *Journal of Applied Polymer Science*, 108(6), 3867–3875.
67. Derawi, D., Salimon, J. (2010). Optimization on epoxidation of palm olein by using performic acid. *Journal of Chemistry*, 7(4), 1440–1448.
68. Tamami, B., Sohn, S., Wilkes, G. L. (2004). Incorporation of carbon dioxide into soybean oil and subsequent preparation and studies of nonisocyanate polyurethane networks. *Journal of Applied Polymer Science*, 92(2), 883–891.
69. Pereira, I. R., D'Abadia, P. L., do Prado, A. D. L., Matos, M. F., Carlos, N. J. et al. (2018). Trends and gaps in the global scientific literature about *Jatropha curcas* L. (Euphorbiaceae), a tropical plant of economic importance. *Semina: Ciências Agrárias*, 39(1), 7–17.
70. Piloto-Rodríguez, R., Tobío, I., Ortiz-Alvarez, M., Díaz, Y., Konradi, S. et al. (2020). An approach to the use of *Jatropha curcas* by-products as energy source in agroindustry. *Energy Sources, Part A: Recovery, Utilization, and Environmental Effects*, 1–21. DOI 10.1080/15567036.2020.1749192.
71. Olcay, H., Kocak, E. D., Yıldız, Z. (2020). *Sourcing synthetic and novel alternative raw materials. Sustainability in polyurethane synthesis and bio-based polyurethanes*. Denmark: Springer Cham.
72. Aristri, M. A., Lubis, M. A. R., Iswanto, A. H., Fatriasari, W., Sari, R. K. et al. (2021). Bio-based polyurethane resins derived from tannin: Source, synthesis, characterisation, and application. *Forests*, 12(11), 1516. DOI 10.3390/f12111516.
73. Saalah, S., Abdullah, L. C., Aung, M. M., Salleh, M. Z., Awang Biak, D. R. et al. (2015). Waterborne polyurethane dispersions synthesized from Jatropha oil. *Industrial Crops and Products*, 64(2), 194–200. DOI 10.1016/j.indcrop.2014.10.046.
74. Liao, L., Li, X., Wang, Y., Fu, H., Li, Y. (2016). Effects of surface structure and morphology of nanoclays on the properties of Jatropha curcas oil-based waterborne polyurethane/clay nanocomposites. *Industrial & Engineering Chemistry Research*, 55(45), 11689–11699. DOI 10.1021/acs.iecr.6b02527.
75. Aung, M. M., Yaakob, Z., Kamarudin, S., Abdullah, L. C. (2014). Synthesis and characterization of Jatropha (*Jatropha curcas* L.) oil-based polyurethane wood adhesive. *Industrial Crops and Products*, 60, 177–185. DOI 10.1016/j.indcrop.2014.05.038.
76. Saravari, O., Praditvatanakit, S. (2013). Preparation and properties of urethane alkyd based on a castor oil/Jatropha oil mixture. *Progress in Organic Coatings*, 76(4), 698–704. DOI 10.1016/j.porgcoat.2012.12.012.

77. Amri, M. R., Al-Edrus, S. S. O., Guan, C. T., Yasin, F. M., Hua, L. S. et al. (2021). Jatropha oil as a substituent for palm oil in biobased polyurethane. *International Journal of Polymer Science*, 2021(5), 1–12. DOI 10.1155/2021/6655936.
78. SaifulAzry, S. O. A., Chuah, T. G., Paridah, M. T., Aung, M. M., Ridzuan, M. A. et al. (2020). Influence of cellulose II polymorph nanowhiskers on bio-based nanocomposite film from Jatropha oil polyurethane. *Materials Research Express*, 8(1), 015003. DOI 10.1088/2053-1591/abc6ce.
79. Cargill (2019). *BiOH® Polyol and Polymer FAQs*. USA: Cargil. <https://www.cargill.com/bioindustrial/bioh-faqs>.
80. Forleo, M. B., Palmieri, N., Suardi, A., Coaloa, D., Pari, L. (2018). The eco-efficiency of rapeseed and sunflower cultivation in Italy. Joining environmental and economic assessment. *Journal of Cleaner Production*, 172, 3138–3153.
81. Fridrihsone, A., Abolins, A., Kirpluks, M. (2020). Screening life cycle assessment of tall oil-based polyols suitable for rigid polyurethane foams. *Energies*, 13(20), 5249. DOI 10.3390/en13205249.
82. Fridrihsone, A., Romagnoli, F., Cabulis, U. (2020). Environmental life cycle assessment of rapeseed and rapeseed oil produced in Northern Europe: A Latvian case study. *Sustainability*, 12(14), 5699. DOI 10.3390/su12145699.
83. Tortoioli, S., Paolotti, L., Romagnoli, F., Boggia, A., Rocchi, L. (2020). Environmental assessment of bio-oil transformation from thistle in the Italian context: An LCA study. *Environmental and Climate Technologies*, 24(3), 430–446. DOI 10.2478/rtuect-2020-0114.
84. Kaikade, D. S., Sabnis, A. S. (2022). Polyurethane foams from vegetable oil-based polyols: A review. *Polymer Bulletin*, 26(19), 1–23. DOI 10.1007/s00289-022-04155-9.
85. Fridrihsone, A., Romagnoli, F., Kirsanovs, V., Cabulis, U. (2020). Life cycle assessment of vegetable oil based polyols for polyurethane production. *Journal of Cleaner Production*, 266(4), 121403. DOI 10.1016/j.jclepro.2020.121403.